JACS
JOURNAL OF THE AMERICAN CHEMICAL SOCIETY

Subscriber access provided by American Chemical Society

Article

Sampling Unfolding Intermediates in Calmodulin by Single-Molecule Spectroscopy

Brian D. Slaughter, Jay R. Unruh, E. Shane Price, Jason L. Huynh, Ramona J. Bieber Urbauer, and Carey K. Johnson

J. Am. Chem. Soc., **2005**, 127 (34), 12107-12114• DOI: 10.1021/ja0526315 • Publication Date (Web): 09 August 2005

Downloaded from http://pubs.acs.org on March 25, 2009

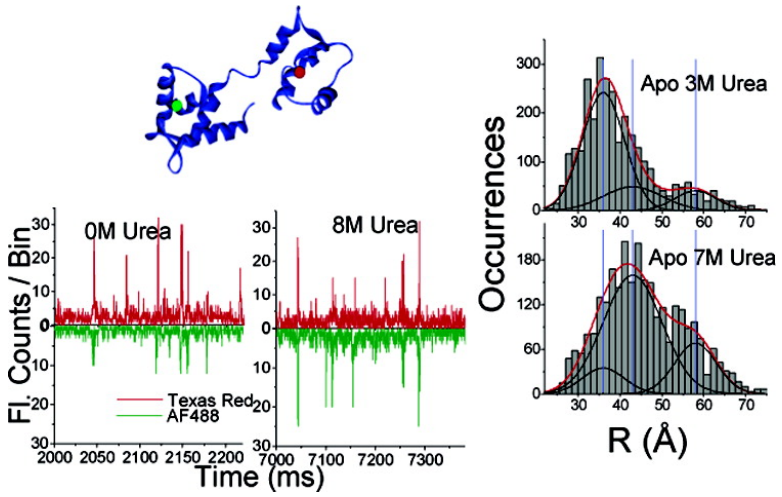

More About This Article

Additional resources and features associated with this article are available within the HTML version:

- Supporting Information
- Links to the 4 articles that cite this article, as of the time of this article download
- Access to high resolution figures
- Links to articles and content related to this article
- Copyright permission to reproduce figures and/or text from this article

View the Full Text HTML

ACS Publications
High quality. High impact.

Journal of the American Chemical Society is published by the American Chemical Society. 1155 Sixteenth Street N.W., Washington, DC 20036

J|A|C|S
ARTICLES
Published on Web 08/09/2005

Sampling Unfolding Intermediates in Calmodulin by Single-Molecule Spectroscopy

Brian D. Slaughter,[‡] Jay R. Unruh,[‡] E. Shane Price,[‡] Jason L. Huynh,[‡] Ramona J. Bieber Urbauer,[§] and Carey K. Johnson*,[‡]

Contribution from the Department of Chemistry, 1251 Wescoe Hall Drive, University of Kansas, Lawrence, Kansas 66045-7582, and the Department of Chemistry and Department of Biochemistry and Molecular Biology, University of Georgia, Athens, Georgia 30602

Received April 22, 2005; E-mail: ckjohnson@ku.edu

Abstract: We used single-pair fluorescence resonance energy transfer (spFRET) measurements to characterize denatured and partially denatured states of the multidomain calcium signaling protein calmodulin (CaM) in both its apo and Ca^{2+}-bound forms. The results demonstrate the existence of an unfolding intermediate. A CaM mutant (CaM-T34C-T110C) was doubly labeled with fluorescent probes AlexaFlour 488 and Texas Red at opposing globular domains. Single-molecule distributions of the distance between fluorophores were obtained by spFRET at varying levels of the denaturant urea. Multiple conformational states of CaM were observed, and the amplitude of each conformation was dependent on urea concentration, with the amplitude of an extended conformation increasing upon denaturation. The distributions at intermediate urea concentrations could not be adequately described as a combination of native and denatured conformations, showing that CaM does not denature via a two-state process and demonstrating that at least one intermediate is present. The intermediate conformations formed upon addition of urea were different for Ca^{2+}-CaM and apoCaM. An increase in the amplitude of a compact conformation in CaM was observed for apoCaM but not for Ca^{2+}-CAM upon the addition of urea. The changes in the single-molecule distributions of CaM upon denaturation can be described by either a range of intermediate structures or by the presence of a single unfolding intermediate that grows in amplitude upon denaturation. A model for stepwise unfolding of CaM is suggested in which the domains of CaM unfold sequentially.

Introduction

Calmodulin (CaM) is a small, Ca^{2+}-binding protein that is involved in signaling pathways for a number of crucial cellular processes, including neurotransmission and muscle contraction.[1,2] CaM is effective in activating a large number of target enzymes, presumably due to the flexibility of the central linker that connects its two Ca^{2+}-binding lobes.[3−5] Single-molecule studies in our laboratory have recently shown that CaM is present in solution in multiple, distinct conformations at room temperature[6,7] that may contribute to the interaction of CaM with targets in diverse binding geometries. We found that the relative amplitudes of these conformations depend on Ca^{2+} level, ionic strength, pH, and oxidative modification with H_2O_2.[7]

The presence of multiple conformations of CaM in solution raises the question of the nature of its folding pathway. The protein-folding pathway of CaM is particularly interesting for a number of reasons. First, the different conformations present at native conditions may fold via distinct folding pathways from either unique or similar unfolded structures at denaturing conditions. Second, the presence of distinct N- and C-terminal domains connected by a central linker raises the possibility of stepwise unfolding, possibly following a hierarchic progression through an unfolding intermediate.[8] The objective of this study is therefore to detect conformational substates of CaM under denaturing conditions and to characterize conformations that appear in the unfolding pathway of CaM by single-pair fluorescence resonance energy transfer (spFRET). The results lead to a proposed unfolding pathway for CaM. While it is generally believed that very small proteins (<100 residues) fold without highly populated intermediate species,[9,10] proteins with a large number of amino acids may follow complex folding pathways. With 148 residues, CaM may possess populated folding intermediates, but its folding pathway should be amenable to detailed study. Thermal and chemical unfolding studies of apoCaM suggested the existence of unfolding intermediates and showed that unfolding of the intact protein cannot be described simply as the sum of the behavior of

[‡] University of Kansas.
[§] University of Georgia.

(1) Hoeflich, K. P.; Ikura, M. *Cell* **2002**, *108*, 739−742.
(2) Persechini, A.; Stemmer Paul, M. *Trends Cardiovasc. Med.* **2002**, *12*, 32−37.
(3) Yamniuk, A., P.; Vogel, H. J. *Mol. Biotechnol.* **2004**, *27*, 33−58.
(4) Weinstein, H.; Mehler, E. L. *Annu. Rev. Physiol.* **1994**, *56*, 213−236.
(5) Baber, J. L.; Szabo, A.; Tjandra, N. *J. Am. Chem. Soc.* **2001**, *123*, 3953−3959.
(6) Slaughter, B. D.; Allen, M. W.; Unruh, J. R.; Urbauer, R. J. B.; Johnson, C. K. *J. Phys. Chem. B* **2004**, *108*, 10388−10397.
(7) Slaughter, B. D.; Unruh, J. R.; Allen, M. W.; Bieber Urbauer, R. J.; Johnson, C. K. *Biochemistry* **2005**, *44*, 3694−3707.
(8) Baldwin, R. L.; Rose, G. D. *Trends Biochem. Sci.* **1999**, *24*, 77−83.
(9) Dobson, C. M. *Nature* **2003**, *426*, 884−890.
(10) Pande, V. S. *Proc. Natl. Acad. Sci. U.S.A.* **2003**, *100*, 3555−3556.

independent N- and C-terminal fragments.[11−15] Small-angle X-ray scattering showed elongation of CaM upon denaturation in urea and suggested the presence of a stable unfolding intermediate of apoCaM at ∼2.5 M urea.[16]

Single-molecule spectroscopy is a valuable method for studying protein folding, due to its ability to characterize heterogeneous systems.[17,18] Previous single-molecule measurements on CaM by Moerner and co-workers have demonstrated FRET in a Ca^{2+}-sensitive chameleon.[19] Lu and co-workers have examined nanosecond domain motions by single-molecule methods,[20] while Hochstrasser and co-workers have observed dynamics of interaction between CaM and an amphiphilic peptide.[21] spFRET is particularly useful in its ability to map out conformational distributions and unveil structural intermediates.[22−25] spFRET has been used to examine conformational changes upon denaturation for a number of proteins, including the cold-shock protein Csp*Tm*,[26] chymotrypsin inhibitor 2,[27] a peptide, GCN4, from the yeast transcription factor,[28] and adenylate kinase.[29]

In the current study, single-molecule conformational distributions were detected for CaM doubly labeled with the FRET pair Alexa Fluor 488 (AF488) and Texas Red (TR) at sites 34 and 110 at varying concentrations of the denaturant urea to elucidate the folding pathway of Ca^{2+}-CAM and apoCaM. In contrast to previous single-molecule unfolding studies on smaller proteins, the single-molecule distributions of CaM at intermediate urea levels cannot be explained simply by a combination of unfolded and folded structures; either a range of intermediate structures or a single unfolding intermediate is required to explain the changes in the conformational distributions of CaM upon unfolding. This provides direct single-molecule evidence of a folding pathway that is not explained by a two-state model. The conformations formed upon addition of urea can be described either by a gradual shift in a compact conformation to a more extended conformation upon unfolding through a range of intermediate structures or by formation of a single folding intermediate.

Materials and Methods

Sample Preparation. CaM-T34C-T110C was expressed by a PCR method described previously.[30,31] CaM-T34C-T110C was purified, labeled simultaneously with AF488 maleimide as donor (D) and TR maleimide as acceptor (A), and separated as described previously.[30,31] Dyes were obtained from Molecular Probes, (Eugene, Or). The double-labeled construct CaM-DA was separated from other species present (i.e., CaM-DD and CaM-AA) by reverse phase HPLC with a C5 Bio Wide Pore column and a standard acetonitrile, water gradient (see Supporting Information in ref 30). The purity of doubly labeled CaM-DA was checked by mass spectrometry (Supporting Information in ref 30). The mass spectrum of CaM-DA[30] verified that the maleimide ring did not open after dye labeling. The functionality of the labeled protein was demonstrated by showing that the doubly labeled construct was able to fully activate the Ca^{2+} pump, PMCA (see Supporting Information). Buffer conditions consisted of 10 mM HEPES, pH 7.4, 0.1 mM Ca^{2+}, 1 mM $MgCl_2$, and 0.1 M KCl. For studies of apoCaM, addition of 300 μM EGTA resulted in free Ca^{2+} concentrations on the order of 150 nM.

Microscope Setup. Fluorescence bursts were collected as described previously[6,7] by exciting freely diffusing molecules with the 488-nm line of an Ar^+ laser (Coherent, Innova 300) and collecting the fluorescence with an inverted fluorescence microscope (Nikon TE2000). The excitation power at the entrance of the objective was 30 μW. A drop of CaM-DA at a concentration of approximately 100 pM was placed on a microscope cover slip above the objective. The beam was focused at a minimum of 20 μm above the surface to reject fluorescence from molecules that may have adhered to the glass surface. Fluorescence was detected in donor and acceptor channels in 300-μs bins.

Analysis of FRET Distributions. The diffusion of a molecule through the focal volume of the microscope was detected by occurrences of high count levels. On the picomolar concentration regime, the probability of a molecule occupying the excitation volume is low; therefore, it was necessary to set threshold signal levels to detect the presence of a CaM molecule in the focal region. Cutoff methods such as those used in these experiments have been discussed in greater detail previously.[6,7,24] For inclusion of a bin in a distribution, it was required that the donor or acceptor counts be larger than 6 times the standard deviation of the background signal in each channel separately or that the sum of donor and acceptor counts be 6 times above the sum of the donor and acceptor background level. These criteria allow for the identification of times when a molecule is present in the focal region without bias between donor and acceptor count channels. Average donor bleed-through into the acceptor channel (roughly 10%) was subtracted from the acceptor counts. It was required that acceptor counts be above background after subtraction of donor bleed-through to avoid inclusion of bins with apparent low FRET efficiency due to acceptor photobleaching.

The actual cutoffs used in a particular experiment are necessarily somewhat arbitrary in nature. However, data analyzed with slightly modified criteria, for example, by increasing or decreasing the number of standard deviations above the background count level a channel must possess, resulted in very similar distributions (see Supporting Information). To ensure that conclusions in the manuscript do not depend on threshold settings, we have (1) collected distributions with identical threshold values to ensure that differences in distributions reflect real differences in conformations and do not depend on the exact value of threshold settings, (2) verified that the average FRET efficiency reported from the distributions matches closely the average FRET efficiency reported from ensemble measurements, which do not involve a threshold setting, and (3) shown previously that ensemble time-resolved fluo-

(11) Sorensen, B. R.; Faga, L. A.; Hultman, R.; Shea, M. A. *Biochemistry* **2002**, *41*, 15−20.
(12) VanScyoc, W. S.; Shea, M. A. *Protein Sci.* **2001**, *10*, 1758−1768.
(13) Sorensen, B. R.; Shea, M. A. *Biochemistry* **1998**, *37*, 4244−4253.
(14) Masino, L.; Martin, S. R.; Bayley, P. M. *Protein Sci.* **2000**, *9*, 1519−1529.
(15) Rabl, C.-R.; Martin, S. R.; Neumann, E.; Bayley, P. M. *Biophys. Chem.* **2002**, *101*−*102*, 553−564.
(16) Yokouchi, T.; Izumi, Y.; Matsufuji, T.; Jinbo, Y.; Yoshino, H. *FEBS Lett.* **2003**, *551*, 119−122.
(17) Moerner, W. E.; Orrit, M. *Science* **1999**, *283*, 1670−1676.
(18) Weiss, S. *Nat. Struct. Biol.* **2000**, *7*, 724−729.
(19) Brasselet, S.; Peterman, E. J. G.; Miyawaki, A.; Moerner, W. E. *J. Phys. Chem. B* **2000**, *104*, 3676−3682.
(20) Tan, X.; Hu, D.; Squier, T. C.; Lu, H. P. *Appl. Phys. Lett.* **2004**, *85*, 2420−2422.
(21) Tang, J.; Mei, E.; Green, C.; Kaplan, J.; DeGrado, W. F.; Smith, A. B., III; Hochstrasser, R. M. *J. Phys. Chem. B* **2004**, *108*, 15910−15918.
(22) Ha, T. *Methods* **2001**, *25*, 78−86.
(23) Dahan, M.; Deniz, A. A.; Ha, T.; Chemla, D. S.; Schultz, P. G.; Weiss, S. *Chem. Phys.* **1999**, *247*, 85−106.
(24) Grunwell, J. R.; Glass, J. L.; Lacoste, T. D.; Deniz, A. A.; Chemla, D. S.; Schultz, P. G. *J. Am. Chem.* Soc. **2001**, *123*, 4295−4303.
(25) Ha, T.; Enderle, T.; Ogletree, D. F.; Chemla, D. S.; Selvin, P. R.; Weiss, S. *Proc. Natl. Acad. Sci. U.S.A.* **1996**, *93*, 6264−6268.
(26) Schuler, B.; Lipman, E. A.; Eaton, W. A. *Nature* **2002**, *419*, 743−747.
(27) Deniz, A. A.; Laurence, T. A.; Beligere, G. S.; Dahan, M.; Martin, A. B.; Chemla, D. S.; Dawson, P. E.; Schultz, P. G.; Weiss, S. *Proc. Natl. Acad. Sci. U.S.A.* **2000**, *97*, 5179−5184.
(28) Talaga, D. S.; Lau, W. L.; Roder, H.; Tang, J.; Jia, Y.; DeGrado, W. F.; Hochstrasser, R. M. *Proc. Natl. Acad. Sci. U.S.A.* **2000**, *97*, 13021−13026.
(29) Rhoades, E.; Gussakvosky, E.; Haran, G. *Proc. Natl. Acad. Sci. U.S.A.* **2003**, *100*, 3197−3202.
(30) Allen, M. W.; Bieber Urbauer, R. J.; Johnson, C. K. *Anal. Chem.* **2004**, *76*, 3630−3637.
(31) Allen, M. W.; Urbauer, R. J. B.; Zaidi, A.; Williams, T. D.; Urbauer, J. L.; Johnson, C. K. *Anal. Biochem.* **2004**, *325*, 273−284.

rescence measurements, which do not depend on threshold settings, result in distance distributions showing conformational substates.[6]

Once it was determined that donor and/or acceptor counts were high enough to ensure that a molecule was present in the focal region, the FRET efficiency for a single bin was found from donor intensity I_d and acceptor intensity I_a using the equation

$$E = \frac{c(I_a - bI_d)}{c(I_a - bI_d) + I_d} \quad (1)$$

where c is a factor to correct for relative detection efficiency of the donor and acceptor channels and b corrects for average bleed-through from the donor to acceptor channel. The determination of c has been discussed in detail elsewhere.[30]

From the FRET efficiency measured in each time bin, distances (R) were obtained according to

$$R = \left(\frac{1 - E}{E}\right)^{1/6} \cdot R_0 \quad (2)$$

where R_0 is the Förster distance, or distance of 50% energy transfer between donor and acceptor. The measured FRET efficiency is an average over the 300-μs time bin. It should be noted that the calculation of distances according to eq 2 does not take into account possible averaging of the FRET efficiency due to dynamics on a time scale faster than the binning time of 300 μs, nor does it correct for contributions from shot noise. For AF488 and TR, a value of 46.5 Å was calculated for R_0 from the equation

$$R_0 = 9.79 \times 10^3 (n^{-4} \kappa^2 \phi_d J)^{1/6} \quad (3)$$

where J is the spectral overlap of the donor fluorescence and acceptor absorption, κ^2 is the orientational dipole−dipole coupling factor, n is the refractive index (1.4), and ϕ_d is the quantum yield of the donor in the absence of the acceptor.[32] A value of $^2/_3$ for κ^2 can be assumed in the current study due to rapid reorientation of AF488, revealed by time-resolved anisotropy measurements (see Supporting Information). The contribution of orientation factors to distance distributions was discussed in previous publications.[6,7] Further discussion, including time-resolved anisotropies of CaM-AF488 and CaM-TR as a function of urea to verify orientational averaging of the orientational factor κ^2, is included in the Supporting Information. As described there, the large amplitude of segmental motion of AF488 ensures random orientation of donor and acceptor dipoles to minimize uncertainty in FRET due to variation in κ^2. At native conditions, some bins were obtained with no detected donor photons leading to a calculated FRET efficiency of 1.0. These cases result from instances of high energy-transfer efficiency coupled with Poisson counting noise in the donor channel. A 100% FRET efficiency corresponds to an apparent R value of 0 Å but could occur for R values less than ca. $^1/_2$ of the Förster distance R_0, or less than 23 Å. Because these cases correspond to an energy-transfer regime in which it is not possible to determine the distance, these occurrences were not included in the distance distributions. It should be noted that, in any case, conformations corresponding to no donor counts were absent in the presence of urea. Use of these cutoff criteria described above resulted in distributions whose average matched the average FRET efficiency obtained from integration of bulk data for CaM at various urea levels (Figure 2 inset, see Results section). Bulk emission spectra were taken upon excitation at 490 nm with a Cary Eclipse fluorimeter, and donor and acceptor emission spectra were numerically integrated in Origin 7.0.

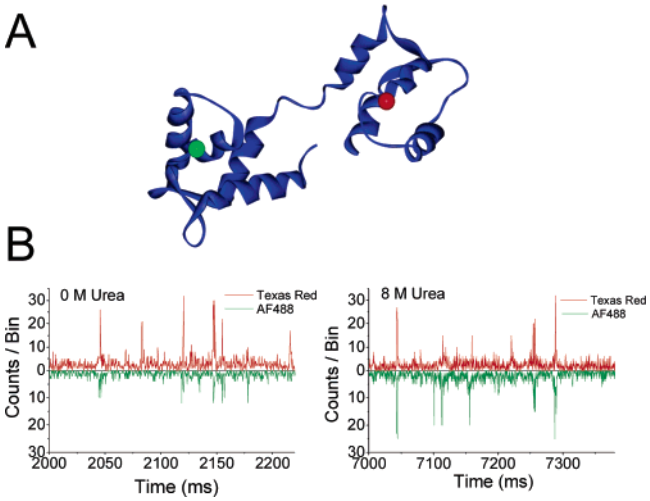

Figure 1. (A) Solution structure of apoCaM (pdb 1cfd[33]) showing the sites of attachment of probes Alexa Fluor 488 (green) and Texas Red (red). (B) Sample fluorescence records of CaM-DA collected in 300-μs bins with excitation of AF 488 at 488 nm. Intense bursts are due to single CaM molecules traversing the focal region. Fluorescence bursts in the acceptor (Texas Red) channel demonstrate efficient FRET. More fluorescence is observed in the donor channel upon addition of urea, indicating decreased FRET.

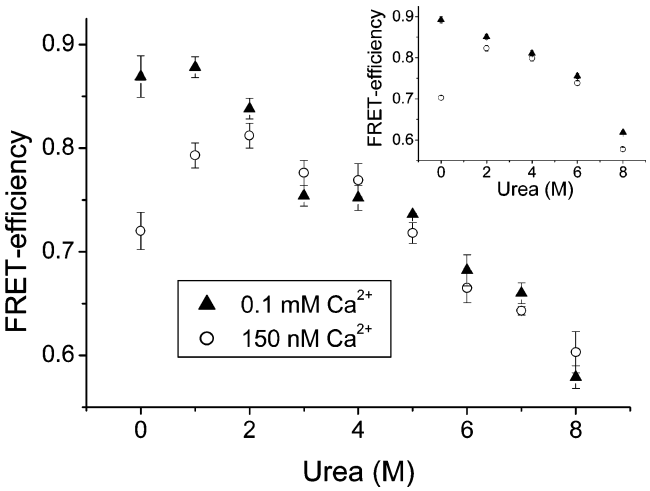

Figure 2. FRET efficiencies as a function of urea concentration averaged over all bins that surpass the signal-to-background criteria for Ca^{2+}-CaM (▲) and apoCaM (○). The uncertainty is the standard deviation in the average from the FRET efficiencies calculated from multiple data sets. The inset shows the average FRET efficiency from ensemble FRET measurements, determined by numerical integration of donor and acceptor peak intensities.

Results

Figure 1A shows a solution structure of apoCaM (pdb 1cfd)[33] and the sites of attachment of fluorescent probes AF488 and TR, and Figure 1B shows two typical data sets with clear examples of high count levels that represent single CaM-DA molecules traversing the focal region. Bursts are shown both at 0 and 8 M urea. There is a notable increase in donor fluorescence for bursts at 8 M urea, evidence of a decrease in FRET efficiency upon denaturation. Data sets were sorted according to the cutoff parameters discussed in Materials and Methods. Figure 2 shows the change in average FRET efficiency upon denaturation of

(32) Van der Meer, B. W.; Coker, G.; Chen, S.-Y. *Resonance energy transfer: theory and data*; VCH: New York, 1994.

(33) Kuboniwa, H.; Tjandra, N.; Grzesiek, S.; Ren, H.; Klee, C. B.; Bax, A. *Nat. Struct. Biol.* **1995**, *2*, 768−776.

CaM by urea for bins exceeding the signal-to-background criteria. To check the validity of the cutoff criteria used, the average FRET efficiency from single-molecule distributions was compared to the average FRET efficiency of bulk measurements. The inset displays the average FRET efficiency of CaM-DA obtained by numerical integration of donor and acceptor emission curves from bulk samples at various urea levels. Comparison shows that the average FRET efficiencies were consistent for the two methods.

The average FRET efficiencies revealed a decreasing FRET efficiency as the urea level increased (with the exception of apoCaM below 2 M urea concentrations), in agreement with X-ray scattering[16] and ensemble FRET studies[34] that observed elongation in the structure of CaM upon addition of urea. The decrease in average FRET efficiency between 2 M urea ($E \approx 0.82$) to 8 M urea ($E \approx 0.60$) was gradual, and the average FRET efficiency between residues 34 and 110 did not appear to depend on Ca^{2+} level over this range of urea concentrations. In contrast, at native conditions, a significant difference existed in the average FRET efficiency of Ca^{2+}-CaM and apoCaM, with average FRET efficiencies for Ca^{2+}-CaM-DA and apoCaM-DA of 0.87 and 0.73, respectively. As the urea level was increased from 0 to 2 M, the average FRET efficiency between residues 34 and 110 in Ca^{2+}-CaM decreased, while it increased for apoCaM at urea concentrations between 0 and 2 M and then decreased between 2 and 8 M urea.

Single-molecule methods allow measurement of the conformational distributions underlying the average FRET efficiencies. Distance distributions at various urea levels are shown in Figure 3, with single-molecule distributions for 0.1 mM Ca^{2+} in the left column and 150 nM Ca^{2+} in the right column. At a Ca^{2+} concentration of 150 nM, we expect CaM to be predominantly in its apo state.[7] Previous single-molecule studies in our laboratory revealed three distinct conformations of Ca^{2+}-CaM and apoCaM at room temperature:[6,7] a dominant conformation consisting of a 30−40 Å distance between residues 34 and 110, an extended conformation with residues 34 and 110 separated by 50−60 Å, and a compact conformation with a distance of ~28 Å between residues 34 and 110. The distributions in Figure 3 are consistent with these findings. Two distinct conformations were apparent in the absence of urea. In the present study, distributions were obtained with a larger bin size of 1.5 Å to demonstrate clearly the changes in the two main conformations upon denaturation, and the most compact conformation was not resolved with bins this large. The amplitudes of the 30−40 and 50−60 Å conformations reported in Figure 3 (top panel) are consistent with those reported previously[7] to within a few percent, consistent with experimental uncertainty.

The results in Figure 3 show that the decrease in average FRET efficiency shown in Figure 2 did not result merely from a shift in the structure of a single population but rather was due to a combination of factors including a shift and broadening of the 30−40 Å distribution and an increase in amplitude of the extended (>50 Å) conformation. Ca^{2+}-CaM and apoCaM responded differently to increases in urea concentration from 0 to 4 M. At 0.1 mM Ca^{2+}, the distribution at 30−40 Å shifted to slightly longer distances along with significant broadening at increasing urea concentrations. The amplitude of the extended conformation (50−60 Å) increased with increasing urea concentration. In contrast, for 150 nM Ca^{2+} the amplitude of the extended conformation decreased with an increase in the urea concentration from 0 to 2 M. The distribution around 30−40 Å did not shift with increasing urea concentrations at urea levels of 4 M or less in apoCaM, but shifted to longer distances at 5 M urea or above.

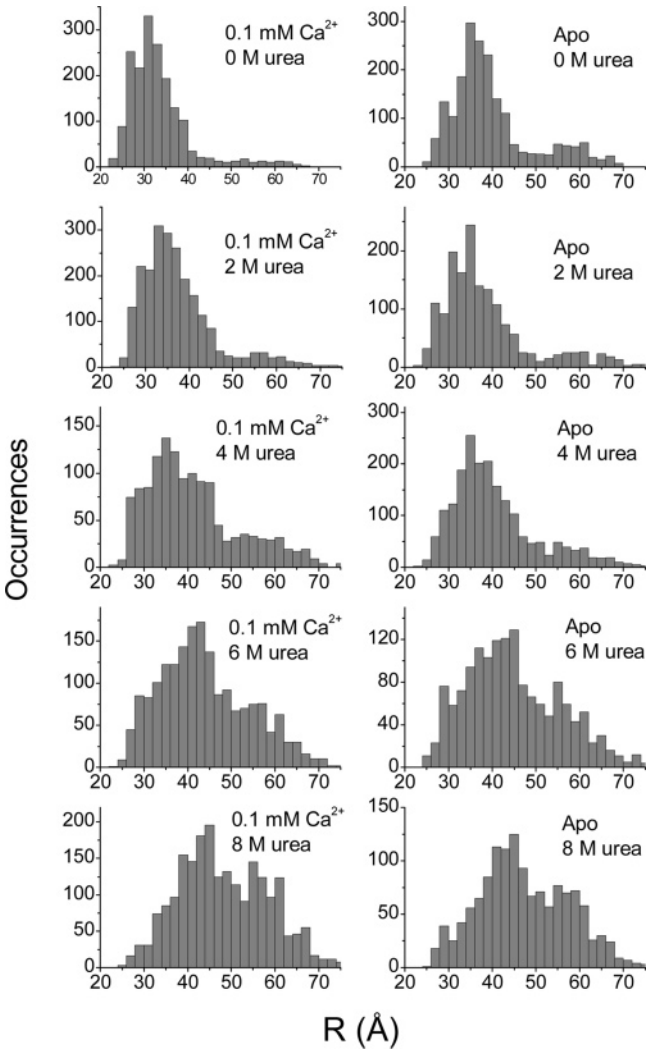

Figure 3. Single-molecule CaM-DA distance distributions at varying urea levels at both saturating (0.1 mM Ca^{2+}, left panel) and subsaturating (150 nM Ca^{2+}, right panel) Ca^{2+} levels. All solutions contain 10 mM HEPES, 0.1 M KCl, and 1 mM $MgCl_2$, pH 7.4. Each histogram comprises approximately 2000 bins corresponding to roughly 1000 single-molecule bursts.

We fit the conformational distributions of Ca^{2+}-CaM and apoCaM in two ways. First, the distributions of distances at various urea concentrations were fit with two Gaussian functions. Examples of such fits are shown in Figure 4. The blue lines in Figure 4 mark the center of the fit for each Gaussian function, while the red lines show the overall fits. The parameters of the fits are plotted in the right column, including the center and width of the shorter-distance Gaussian function and the relative amplitude of the extended-distance Gaussian function. The fits illustrate observations made above. For Ca^{2+}-CaM, the center of the more compact Gaussian shifted upon addition of urea, while for apoCaM the center was relatively unchanged from 0 to 5 M urea before increasing from 5 to 8 M urea. The width of this Gaussian increased upon denaturation for both Ca^{2+}-CaM and apoCaM. As count rates for CaM at

(34) Yao, Y.; Schoeneich, C.; Squier, T. C. *Biochemistry* **1994**, *33*, 7797−7810.

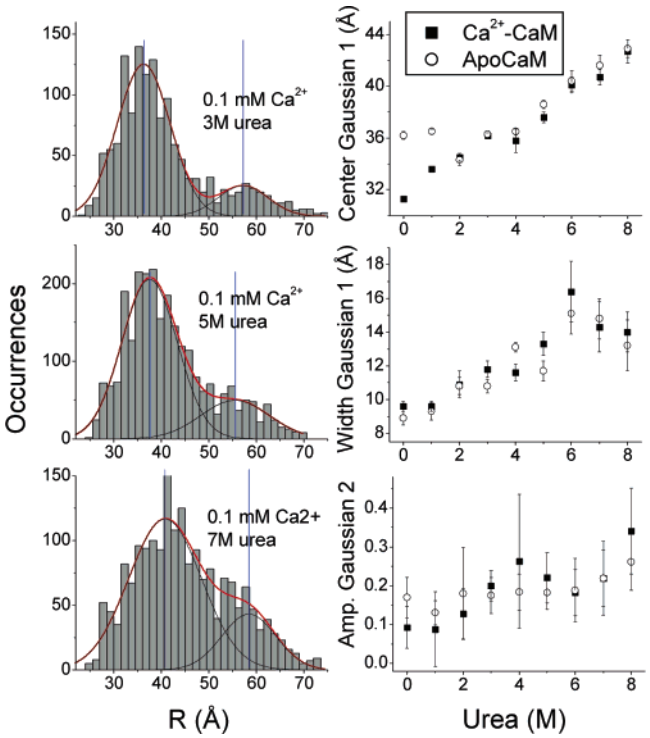

Figure 4. Fits of single-molecule CaM-DA distance distributions to two Gaussian functions, consistent with a broad distribution of intermediate unfolding states (see text). The fits of the individual Gaussians are shown in black and the overall fit in red. Blue lines are drawn to show the center of each of the two components of the fit. Plotted on the right are the center distance and width of the more-compact Gaussian function, along with the relative amplitude of the more extended Gaussian function as a function of urea concentration.

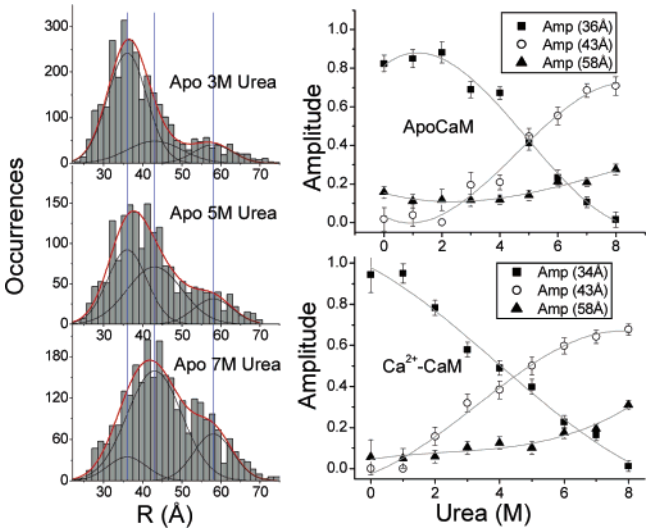

Figure 5. Fits of single-molecule CaM-DA distance distributions to three Gaussian functions with fixed centers and widths. This model is consistent with the existence of a distinct unfolding intermediate represented by the intermediate Gaussian function centered around 43 Å for both apoCaM and Ca^{2+}-CaM. The center and width of each Gaussian were held constant, and only the amplitudes were varied. The fits of the individual Gaussians are shown in black and the overall fit in red. Blue lines are drawn to show the center of each of the three components of the fit. On the right the amplitudes of the three components are plotted as a function of urea concentration at both Ca^{2+} levels. Lines are shown to guide the eye.

increasing urea levels were similar to count rates at native conditions, Poisson counting noise was expected to contribute equally to the width of all distributions, and the increase in width of the distributions upon denaturation was therefore not a result of counting noise. With the exception of apoCaM at less than 2 M urea, there was a trend toward increasing amplitude of the 50−60 Å conformation upon denaturation, while the center of the more extended Gaussian did not shift appreciably in distance.

The shift and broadening of the distributions upon denaturation demonstrate the presence of one or more intermediate states. The simplest description of these states is given by a model with a single folding intermediate. To test this possibility, we fit the distributions with three conformations of fixed center and width, allowing only their amplitudes to vary at different urea concentrations. The center and width of the most compact distribution were found from a fit of the compact distributions (all bins < 45 Å) at native conditions. The parameters for the more extended conformations were found from a fit of the distributions at 8 M urea, yielding peaks at 43 and 58 Å. The distributions at each urea level were then fit to three Gaussian distributions allowing only the amplitudes of the three to vary while fixing the center and width. At 8 M urea an amplitude of <2% was obtained for the distribution centered at 34 Å, so that the distribution was effectively fit with amplitude from the other two Gaussians. However, all three substates were significantly populated at intermediate urea levels. These results are shown in Figure 5. The blue lines mark the fixed centers of the three distributions. The individual Gaussian profiles are also shown, along with the overall fits in red. Plotted on the right side of Figure 5 are the amplitudes of the three populations as a function of urea concentration for apoCaM and Ca^{2+}-CaM.

The fits in Figure 5 illustrate differences in the unfolding of apoCaM and Ca^{2+}-CaM. The amplitude of the 30−40 Å distribution decreased monotonically with increasing urea for Ca^{2+}-CaM. However, for apoCaM, the amplitude of the most compact of the three distributions changed little in amplitude from the native distribution to the distribution at 2 M urea before decreasing at higher urea concentrations. The amplitude of the Ca^{2+}-CaM conformational substate centered at 43 Å grew for urea concentrations between 1 and 6 M before leveling off. For apoCaM, the amplitude of the intermediate conformation changed little between 0 and 2 M urea before increasing to match Ca^{2+}-CaM between 5 and 8 M urea. The amplitude of the 50−60 Å distribution did not change as significantly as the others at low urea levels but increased between 5 and 8 M urea. Interestingly, for apoCaM this amplitude was larger at native conditions than at 1 M urea and increased slowly upon further addition of urea, although it is possible that the physical characteristics of the 50−60 Å conformation of apoCaM at native conditions were different from those of the 50−60 Å population at high urea levels (see Discussion below).

Discussion

Protein folding and unfolding are dynamically and structurally heterogeneous processes. To fold, the protein configuration must find its way along the energy surface to form the native structure. Multiple, local minima may exist on this surface that can trap the protein temporarily in intermediate folding structures.[8] Such structures may be stabilized in the presence of urea. Ensemble measurements typically report only an average physical property and therefore may miss shifts in underlying distributions or intermediate states. Single-molecule methods, on the other hand, reveal the distribution of properties that, taken as a group,

comprise the average. In the current study, changes in the single-molecule distributions of CaM were observed upon denaturation. The single-molecule distributions provide direct evidence for a folding pathway that possesses at least one and possibly a range of intermediate structures.

Previous single-molecule folding measurements of smaller proteins and peptides, chymotrypsin inhibitor 2,[27] cold shock protein from *Thermotoga maritime*,[26,35] and a two-stranded coiled coil from GCN4[28] were consistent with two-state unfolding in which a folded conformation was observed at native conditions and an unfolded conformation at high denaturant levels. At intermediate denaturant concentrations, the single-molecule distributions could be explained as a mixed population of folded and unfolded components. Larger proteins, on the other hand, might be expected to possesses more complicated folding pathways.[36,37] Haran and co-workers observed heterogeneous folding pathways in fluorescence traces of single adenylate kinase molecules (214 amino acids), and distributions at intermediate denaturation concentrations showed states that were shifted slightly from the native and fully denatured states.[29]

Unfolding Models. In the present experiments, the observation of shifts in the compact conformation of CaM upon denaturation demonstrates that the distributions of CaM in the presence of urea cannot be described by the presence of only two populations, one folded and the other unfolded. Rather, we detected shifts and broadening in the more compact conformation, inconsistent with two-state behavior. Therefore, in contrast to a two-state folding mechanism, the folding landscapes of both apoCaM and Ca^{2+}-CaM possess, at a minimum, at least one significantly populated intermediate structure between native and unfolded states. The presence of distinct conformations for data recorded in 300-μs bins indicates that the conformations interchange on a time scale of longer than 300 μs. The presence of distinct conformations on this time scale is consistent with a kinetic study of Bayley and co-workers, who observed equilibration between native and unfolded conformations of the C-domain of apoCaM on the time scale of hundreds of microseconds.[15]

The shifts in conformational distributions with addition of urea can be understood in two alternative pictures. First, the distributions can be explained by a shift and broadening of the more compact conformation along with an increase in amplitude of an extended 50−60 Å conformation. Distributions fit with two Gaussian functions are shown in Figure 4. In the context of this model, the shift and broadening of the 30−40 Å conformation suggests that CaM may form a continuous distribution of intermediate unfolding states. Such a distribution of unfolding states would be consistent with a downhill folding mechanism along a surface void of significant barriers, with a range of accessible conformations that decreases in number as the native structure stabilizes.[38−41] The shift and broadening of the 30−40 Å conformation could result from disruption of one set of hydrogen bonds, while disruption of another set of hydrogen bonds could lead to the increase in amplitude of the extended conformation, for example by unfolding of the central linker.

The single-molecule distributions admit a second possible interpretation in which a single unfolding intermediate is formed rather than a range of intermediates. In this picture, the increased breadth of the distributions at intermediate urea concentrations is due to two overlapping conformations. According to this model, there are three populations of CaM: a relatively compact conformation (centered at 34 Å for Ca^{2+}-CaM and 36 Å for apoCaM), an intermediate conformation appearing upon addition of urea (centered at 43 Å for both Ca^{2+}-CaM and apoCaM), and a weakly populated, extended structure (centered at 58 Å). The changes in the distributions with changes in urea concentration can be described by changes in the amplitudes of these conformations. Examples of fits in the context of this model are shown in Figure 5. In this model a folding intermediate centered at 43 Å is evident as its population grows in amplitude and dominates the distribution at high urea levels.

Unfolding Pathways of CaM. CaM possesses unique structural properties that may dictate the nature of the unfolding pathways available. CaM is a structurally flexible protein, as evidenced by its multiple conformations even in the absence of denaturant.[6,7] The N- and C-terminal lobes of CaM have distinct physical characteristics,[3,42−44] including reduced stability in the C-terminal domain of apoCaM relative to that in the N-terminal domain.[13,45] The two lobes are known to interact, affecting characteristics such as flexibility and Ca^{2+} binding.[13,46] Shea and co-workers showed that the isolated domains of apoCaM display two-state unfolding, but a three-state model was necessary to adequately fit the thermal denaturation curve for the intact protein.[13] Bayley and co-workers similarly observed that the unfolding of the whole protein cannot be described simply by a superposition of the unfolding of the two isolated domains.[14] Denaturation of the C-terminal fragment of apoCaM was observed at lower concentration of denaturant than denaturation of the N-terminal fragment of apoCaM, while the order was reversed for Ca^{2+}-CaM.[14] The instability of the C-terminal domain of apoCaM was also observed in a temperature-jump study of the unfolding of apoCaM by Bayley and co-workers, who concluded that the C-domain was partially unfolded at native conditions.[15] These findings suggest that CaM unfolds in a stepwise fashion. One possibility, therefore, is that the observed intermediate consists of CaM in which one of the two terminal domains is denatured.

The observation of the large amplitude of the most compact of the conformations at native conditions, and the increase in amplitude first of the conformation centered ~43 Å, followed by the increase in amplitude of the most extended conformation (Figure 5), indicate that the unfolding of CaM is hierarchic, following a stepwise progression through at least one intermediate structure. These results suggest a simple hypothesis for the

(35) Rhoades, E.; Cohen, M.; Schuler, B.; Haran, G. *J. Am. Chem. Soc.* **2004**, *126*, 14686−14687.
(36) Zhang, H. j.; Sheng, X. R.; Pan, X. M.; Zhou, J. M. *Biochem. J.* **1998**, *333*, 401−405.
(37) Ruan, Q.; Ruan, K.; Balny, C.; Glaser, M.; Mantulin, W. W. *Biochemistry* **2001**, *40*, 14706−14714.
(38) Sabelko, J.; Ervin, J.; Gruebele, M. *Proc. Natl. Acad. Sci. U.S.A.* **1999**, *96*, 6031−6036.
(39) Garcia-Mira, M. M.; Sadqi, M.; Fischer, N.; Sanchez-Ruiz, J. M.; Munoz, V. *Science* **2002**, *298*, 2191−2195.
(40) Oliva, F. Y.; Munoz, V. *J. Am. Chem. Soc.* **2004**, *126*, 8596−8597.
(41) Bryngelson, J. D.; Onuchic, J. N.; Socci, N. D.; Wolynes, P. G. *Proteins: Struct., Funct., Genet.* **1995**, *21*, 167−195.
(42) Martin, S. R.; Bayley, P. M. *Biochem. J.* **1986**, *238*, 485−490.
(43) Barton, N. P.; Verma, C. S.; Caves, L. S. D. *J. Phys. Chem. B* **2002**, *106*, 11036−11040.
(44) VanScyoc, W. S.; Sorensen, B. R.; Rusinova, E.; Laws, W. R.; Ross, J. B. A.; Shea, M. A. *Biophys. J.* **2002**, *83*, 2767−2780.
(45) Browne, J. P.; Strom, M.; Martin, S. R.; Bayley, P. M. *Biochemistry* **1997**, *36*, 9550−9561.
(46) Sun, H.; Yin, D.; Squier, T. C. *Biochemistry* **1999**, *38*, 12266−12279.

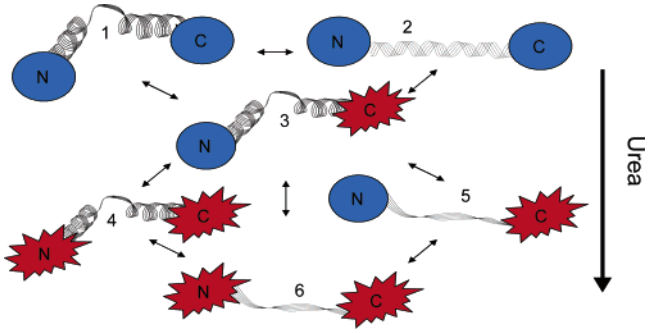

Figure 6. Schematic of possible unfolding pathways of CaM. Structure **1** is the dominant conformation and **2** is the most extended conformation in the absence of urea. Addition of urea leads to formation of a partially denatured structure (**3**) where one of the two terminal domains is denatured (e.g. the C-terminal domain for apoCaM). Native domains are represented by circles and denatured domains are represented by irregular shapes. Upon increasing the urea concentration, structure **3** dominates the distribution. Further increases in urea concentration may denature the opposing globular domain (structure **4**) or the central linker (structure **5**). Eventually, as the urea level is increased, an extended conformation is formed that may correspond to structures **5** or **6**, or a combination of the two. For Ca^{2+}-CaM, structures **2** and **3** are weakly populated at native conditions, whereas for apoCaM, structures **1**, **2**, and **3** are all present at native conditions. Upon addition of urea, structure **3** begins to dominate. For Ca^{2+}-CaM, the N-terminal domain may denature more readily, while the C-terminal domain denatures more readily for apoCaM.[14]

three-state unfolding of CaM in which denaturation in one lobe of CaM at low levels of urea populates an unfolding intermediate with a distance between residues 34 and 110 distributed around 43 Å. Denaturation in the other terminal domain (or denaturation of the central linker—see below) may be responsible for the further increase in the distance between the residues, resulting in additional amplitude for the 50−60 Å conformation.

Possible unfolding pathways of Ca^{2+}-CaM and apoCaM are illustrated in Figure 6. CaM is present in at least three conformations at native conditions.[6,7] Of these, the two most populated conformations are represented in Figure 6 by structures **1** and **2**. Structure **1** represents the dominant conformation, while **2** represents the more extended conformation. We suggest that unfolding of CaM proceeds stepwise through an unfolding intermediate where one of the two terminal domains is denatured. Structure **3** represents an intermediate with a single unfolded domain, which could be the C-terminal domain for apoCaM and the N-terminal domain for Ca^{2+}-CaM.[14] Upon increasing denaturant concentration, the population of structure **3** is increased. Further unfolding occurs either by denaturation of the second domain (the N-terminal domain for apoCaM or the C-terminal domain for Ca^{2+}-CaM) represented by structure **4**, or of the central linker as represented by structure **5**, or of both (structure **6**), increasing the population of an extended conformation (R > 50 Å).

The differences observed in the response of apoCaM and Ca^{2+}-CaM to urea further suggest that a difference exists in their unfolding pathways. The unfolding of Ca^{2+}-CaM results in a gradual increase in the amplitude of the extended formation. In contrast, the results in Figure 5 suggest that an extended conformation of apoCaM is more favored at native conditions relative to slightly denaturing conditions at 2 M urea. Unfolding of apoCaM at low urea concentrations may result in a conformation where, as one domain unfolds, enhanced interactions between domains result in formation of a compact conformation, resulting in a reduced amplitude of the extended conformation. Such interactions could result from exposure of hydrophobic surfaces upon unfolding that are then available to interact with the opposing domain.

It is interesting to consider the nature of the extended conformation (R > 50 Å). The extended conformation in native CaM very likely consists of a helical central linker as depicted by crystal structures of Ca^{2+}-CaM,[47−49] whereas the extended conformation formed upon addition of urea may consist of a denatured central linker. The extended conformation formed under denaturing conditions may thus consist of structures **5** or **6** (Figure 6) or a mixture of both. For apoCaM the population of the extended conformation first decreases upon addition of urea. At urea concentrations above 2 M, the 50−60 Å conformation for apoCaM again grows in population, suggesting that the extended conformation of CaM that grows in amplitude upon denaturation has different structural characteristics than the extended conformation at native conditions. However, more detailed analysis of the structures of the conformational substates is not possible from the present data.

Even though the distance between residues 34 and 110 in the extended conformation of CaM (50−60 Å) appears consistent with the distance predicted by the extended helical crystal structures of Ca^{2+}-CaM (∼53 Å-from pdb 1cll,[49] ∼52 Å for pdb 1exr[47]), it is unlikely that the extended conformation that grows in amplitude at increasing urea levels corresponds to increased helicity in the linker, as ensemble studies have shown a decrease in helicity of CaM upon denaturation.[13,14] Therefore, we speculate that the extended structures of Ca^{2+}-CaM and apoCaM at native conditions have physical characteristics that differ from the extended conformation upon denaturation but that are not manifested as a distance change between residues 34 and 110.

This result can be considered in light of recent simulations that suggest that end-to-end distances in denatured proteins may not differ substantially from end-to-end distances for proteins maintaining specific structural features.[50−52] Pande and co-workers reported that the average end-to-end distance for a random chain differs only slightly from the average end-to-end distance for a helical segment over short distances.[50] Rose and co-workers found that mean-squared end-to-end distances were similar to random-coil predictions for proteins that had only 8% of the torsion angles randomized, while 92% retained their values from the structural data.[53] For a protein chain of 76 residues (the chain length between residues 34 and 110 of CaM) random-coil models predict a mean-squared end-to-end distance of 5351 Å^2.[51,54] (A slightly larger distance might be expected between residues 34 and 110 of CaM due to excluded volume effects for residues in the protein interior.[54]) For comparison to these predictions, we calculated the mean-squared end-to-end distance for the extended 50−60 Å conformation from the Gaussian fit to this population (see Figures 3 and 4). The resulting mean-squared distance of 3500 ± 300 Å^2 is signifi-

(47) Wilson, M. A.; Brunger, A. T. *J. Mol. Biol.* **2000**, *301*, 1237−1256.
(48) Babu, Y. S.; Bugg, C. E.; Cook, W. J. *J. Mol. Biol.* **1988**, *204*, 191−204.
(49) Chattopadhyaya, R.; Meador, W. E.; Means, A. R.; Quiocho, F. A. *J. Mol. Biol.* **1992**, *228*, 1177−1192.
(50) Zagrovic, B.; Pande, V. S. *Nat. Struct. Biol.* **2003**, *10*, 955−961.
(51) Fitzkee, N. C.; Rose, G. D. *Proc. Natl. Acad. Sci. U.S.A.* **2004**, *101*, 12497−12505.
(52) Millett, I. S.; Doniach, S.; Plaxco, K. W. *Adv. Protein Chem.* **2002**, *62*, 241−262.
(53) Fitzkee, N. C.; Rose, G. D. *Proc. Natl. Acad. Sci. U.S.A.* **2004**, *101*, 12497−12502.
(54) Zhou, H.-X. *J. Phys. Chem. B* **2002**, *106*, 5769−5775.

cantly less than the values reported from the random-coil simulations. This comparison strongly suggests that even in the presence of 8 M urea, the extended CaM conformation retains native structural elements and is not adequately described as a random coil between residues 34 and 110.

Another interesting feature of the distributions for both apoCaM and Ca^{2+}-CaM concentrations is that the extended 50−60 Å conformation does not dominate the distribution, even at 8 M urea. The distribution of distances is quite broad and includes a substantial population of compact conformations. This result suggests that denatured structures of CaM tend to retain a large degree of compact structural elements and is consistent with studies that show that CaM is not completely unfolded at 8 M urea.[16] Unfolding simulations by Pandé and co-workers have shown the presence of nativelike mean conformations of three polypeptides in an unfolded state.[55] The presence here of a large population of molecules having structures that are not fully extended averaged over 300 μs bins suggests that both Ca^{2+}-CaM and apoCaM retain structural elements that resemble native conformations, even under unfolding conditions. This observation is also consistent with the report of long-range structure in denatured staphylococcal nuclease.[56−58]

Conclusions

Single-molecule conformational distributions have demonstrated the existence of complex unfolding pathways of both apoCaM and Ca^{2+}-CaM. We have detected the existence of at least three conformational states of apoCaM and Ca^{2+}-CaM at each urea concentration. Diagnosis of the folding pathway for multidomain, structurally heterogeneous proteins such as CaM will be an important step in understanding the process of protein folding. spFRET measurements between AF488 and TR at residues 34 and 110 presented here show that the unfolding pathways of both apoCaM and Ca^{2+}-CaM involve at least one intermediate structure. Furthermore, the results show that changes in the FRET efficiency of CaM upon the addition of urea are due to shifts in the populations of underlying conformational states that are present in native CaM. The finding that even under highly denaturing conditions the conformational distributions still include compact conformations not only underscores the conformational heterogeneity of CaM in its unfolded state but also suggests the retention of structural features that engender less than fully extended conformations, even under denaturing conditions.

The results can be understood in the context of two alternative models of the protein folding pathway. One entails a range of intermediate structures, suggesting a downhill folding progression for CaM. The domain structure of CaM, however, suggests that a distinct unfolding intermediate might exist in the unfolding pathway of CaM in which either the C- or N-terminal domain of CaM is denatured, while the other domain remains in its native conformation. Therefore, we favor a second, simpler model consisting of a single unfolding intermediate characterized by a separation of ∼43 Å between donor and acceptor fluorophores. This unfolding intermediate grows in amplitude and dominates the distribution at high urea levels. This intermediate structure may consist of one unfolded domain of CaM, leading to an increase in distance between lobes of CaM from ∼34 to ∼43 Å. Continued denaturation, possibly involving the linker region, is likely responsible for populating the 50−60 Å conformation. In either picture, however, it is clear that the unfolding pathway for both apoCaM and Ca^{2+}-CaM consists of one or more stable unfolding intermediates.

Acknowledgment. We thank W. E. Moerner for pointing out the connection with molecular dynamics simulations and W. Eaton for suggesting the relationship to mean-squared random coil distances. We thank Dr. Asma Zaidi for measurement of the activity of CaM-DA (see Supporting Information). This research was supported by NIH Grant ROI GM58715. B.D.S. and J.R.U. acknowledge support from the Dynamic Aspects of Chemical Biology NIH Training Grant (NIH 5 T32 GM08545-09). E.S.P. acknowledges support from the Pharmaceutical Aspects of Technology training grant (NIH GM08259).

Supporting Information Available: Controls that were completed to ensure that there was no misinterpretation of single-molecule data due to dye labeling, dye-orientation effects, changes in dye−protein interaction, dye photophysics upon CaM denaturation, or the settings of threshold levels. This material is available free of charge via the Internet at http://pubs.acs.org.

JA0526315

(55) Zagrovic, B.; Snow, C. D.; Khaliq, S.; Shirts, M. R.; Pande, V. S. *J. Mol. Biol.* **2002**, *323*, 153−164.
(56) Shortle, D.; Ackerman, M. S. *Science* **2001**, *293*, 487−489.
(57) Ackerman Michael, S.; Shortle, D. *Biochemistry* **2002**, *41*, 13791−13797.
(58) Dyson, H. J.; Wright, P. E. *Adv. Protein Chem.* **2002**, *62*, 311−340.